Experimental Investigation on the Effect of Heat Transfer Fluid in a Finned-tube Heat Exchanger with a Phase Change Material

Ewelina Radomska[a], Wojciech Kalawa[a], Łukasz Lis[a], Andrzej Gołdasz[a], Marta Kuta[a], Łukasz Mika[a], Agata Mlonka-Mędrala[a], Artur Szajding[b] and Karol Sztekler[a]

[a] AGH University of Krakow, Faculty of Energy and Fuels, Department of Thermal and Fluid Flow Machines, Krakow, Poland, radomska@agh.edu.pl (CA), kalawa@agh.edu.pl, llis@agh.edu.pl, goldasz@agh.edu.pl, marta.kuta@agh.edu.pl, lmika@agh.edu.pl, amlonka@agh.edu.pl, sztekler@agh.edu.pl

[b] AGH University of Krakow, Faculty of Metals Engineering and Industrial Computer Science, Department of Heat Engineering and Environment Protection, Krakow, Poland, artur.szajding@agh.edu.pl

Abstract:

Thermal energy storage (TES) systems play an important role in improving the reliability, flexibility, and efficiency of modern energy infrastructures, particularly those based on renewable energy sources. Among TES technologies, latent heat storage using phase change materials (PCMs), especially solid-liquid ones, has attracted significant attention due to its high energy storage density and ability to operate within a narrow temperature range, enabling compact system designs and reduced thermal losses. However, the generally low thermal conductivity of most PCMs remains a major challenge, as it limits heat transfer rates, prolongs charging and discharging times, and reduces the achievable power output of latent heat storage systems. Therefore, the operating conditions of the heat transfer fluid (HTF) circulating through the heat exchanger are important factors influencing the performance of PCM-based TES units. This study presents an experimental investigation of the influence of three HTF flow rates on the performance of two finned-tube heat exchanger configurations in a PCM-based TES system. The system employed 10 kg of a commercial PCM (A82, Phase Change Material Products Limited, UK) stored in a stainless-steel tank equipped with an internal copper HTF tube. Two heat exchanger configurations were examined: one with fourteen straight alumina fins and another with twenty-one straight alumina fins combined with lowered HTF tubes. Water was used as the HTF at flow rates of 2.4 L/min, 4.7 L/min, and 9.4 L/min, corresponding to average flow velocities of 0.5 m/s, 1.0 m/s, and 2.0 m/s, respectively. The performance of the TES system was evaluated based on PCM temperature evolution and thermal power during charging and discharging processes. The results show that the construction of the heat exchanger affects the TES performance more than changing the HTF flow rate.

Keywords:

Heat exchanger; Latent heat; Phase change material; Thermal energy storage

1. Introduction

Nowadays, thermal energy storage (TES) technologies have become increasingly important due to the growing share of renewable energy sources (RES) and the need to improve the efficiency and flexibility of energy systems [1]. Among various TES solutions, phase change materials (PCMs), particularly solid–liquid PCMs, are considered one of the most promising options. These materials store thermal energy in the form of latent heat during melting and release it during the reverse process of solidification.

Compared to sensible heat storage systems and other types of PCMs, solid–liquid PCMs offer several advantages, including high energy storage density and nearly constant phase change temperature [2]. However, a significant limitation of PCMs is their relatively low thermal conductivity, which leads to slow charging and discharging processes in TES systems [3]. To address this issue, various enhancement techniques have been proposed, such as incorporating thermally conductive additives [4], optimizing heat exchanger designs [5], and modifying operating conditions, including the flow rate and temperature of the heat transfer fluid (HTF) [6].

For instance, Herbinger and Groulx [7] experimentally investigated the effect of the number of fins in a vertical finned tube-and-shell PCM-based TES system. They analyzed configurations with 4, 8, and 12 finned tubes and demonstrated that the heat transfer rate increased with the number of fins due to the enlarged heat transfer

surface area. Similar conclusions were reported by Niu et al. [8] based on numerical simulations. In addition to geometric modifications, the operating parameters of the HTF, such as its temperature and flow rate, influence the performance of PCM-based heat exchangers. Fan et al. [9] examined the effect of HTF inlet temperature in a shell-and-tube PCM-based TES unit and found that increasing the inlet temperature from 70 °C to 80 °C reduced the charging time from approximately 6 hours to 2 hours. Meanwhile, Lv et al. [10] investigated the influence of HTF flow rate and reported that increasing the flow rate from 5 L/min to 15 L/min resulted in a 2.65-fold increase in charging power and a 2.36-fold increase in discharging power. However, several studies indicate that the benefits of increasing HTF flow rate are limited. Panchabikesan et al. [11] observed that beyond a certain threshold, further increases in flow rate lead to diminishing reductions in charging time. Similarly, Shen et al. [12] reported that the performance of PCM-based heat exchangers is generally more sensitive to HTF temperature than to its flow rate.

In this context, the present study aims to experimentally investigate the effect of HTF flow rate on the performance of two PCM-based TES units equipped with different heat exchanger designs. The objectives of this work are threefold. First, to evaluate the thermal performance of the designed heat exchangers. Second, to identify potential operational issues associated with PCM-based TES systems. Third, to provide a basis for further design modifications and performance improvements of PCM-based TES units.

2. Methodology

The experimental setup is schematically shown in **Figure 1**. The setup consisted of the heat exchanger enclosed within a housing and filled with PCM, a hot water buffer tank, a cold water buffer tank, an electric heater, a cooler, pumps, a three-way valve, and appropriate measuring devices, which are listed in **Table 1**. The temperatures of the PCM inside the heat exchanger were measured at twelve locations (**Figure 2**). In addition, the inlet and outlet temperatures of the heat transfer fluid (HTF), as well as its flow rate, were monitored.

Water was used as the HTF during both the charging and discharging processes. The HTF temperature during charging and discharging was set to 97 ± 1 °C and 50 ± 1 °C, respectively. The HTF flow rates were 2.4 L/min, 4.7 L/min, and 9.4 L/min, corresponding to average velocities of 0.5 m/s, 1.0 m/s, and 2.0 m/s, respectively. A82 (PCM Products Ltd., Great Britain), with a melting temperature of 82 °C and a latent heat of fusion of 240 kJ/kg [13], was used as the PCM. The mass of PCM in the heat exchanger was 10 kg.

The experiment started with the charging process, which was considered complete when the lowest measured PCM temperature reached 92 °C. Subsequently, the discharging process was initiated and considered complete when the highest measured PCM temperature dropped to 70 °C. The charging-discharging cycle was repeated three times to ensure repeatability, and the average values were then calculated.

The experiments were conducted using two heat exchangers. The first heat exchanger, hereafter referred to as A (**Figure 3**), featured fourteen straight alumina fins. The second heat exchanger, hereafter referred to as D (**Figure 4**), featured twenty-one straight alumina fins combined with HTF tubes lowered by 15 mm.

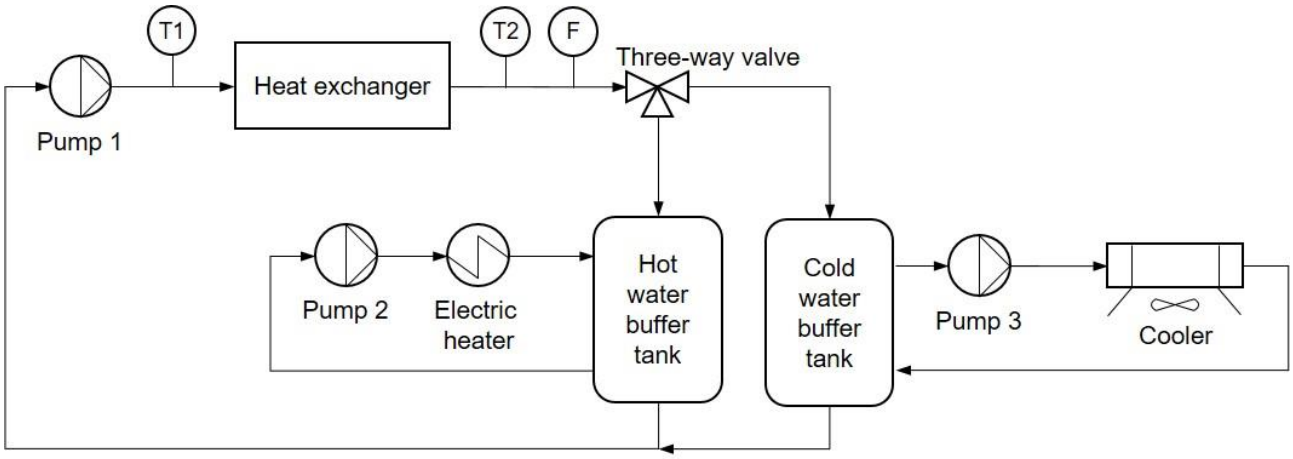

Figure 1. *The diagram of the experimental setup. T – temperature sensor; F – flow rate sensor.*

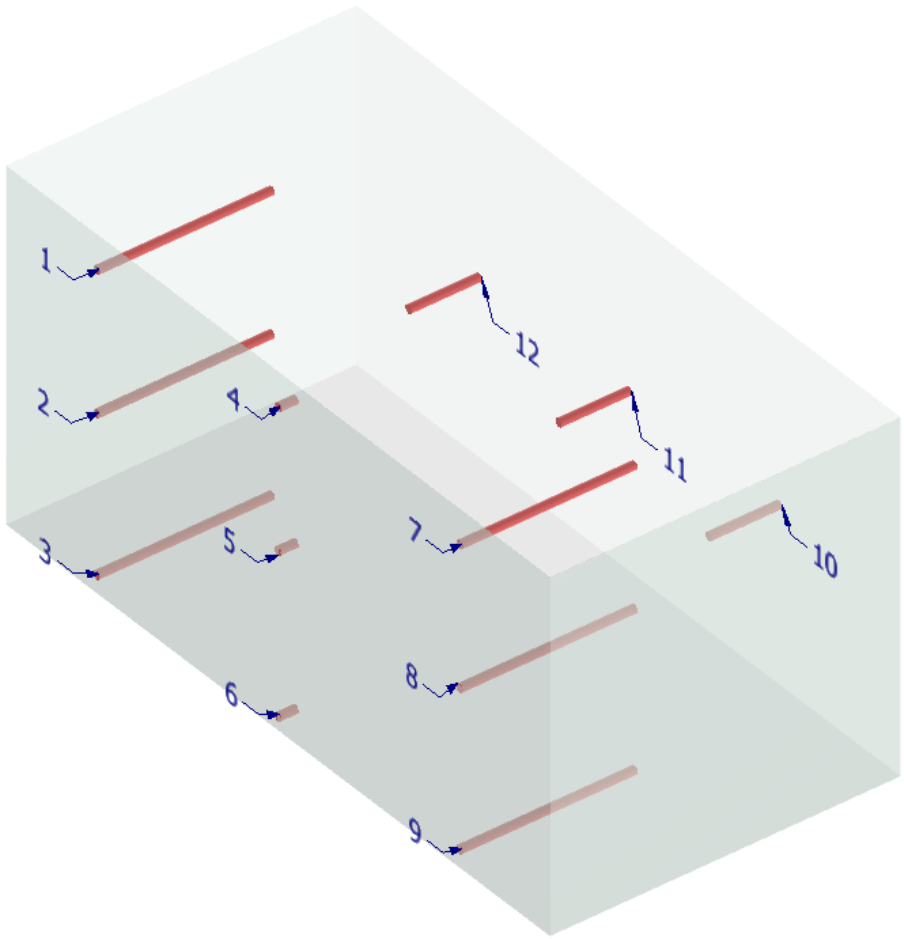

Figure 2. *Location and labelling of temperature sensors inside the thermal energy storage (schematic diagram – scale and dimensions not shown).*

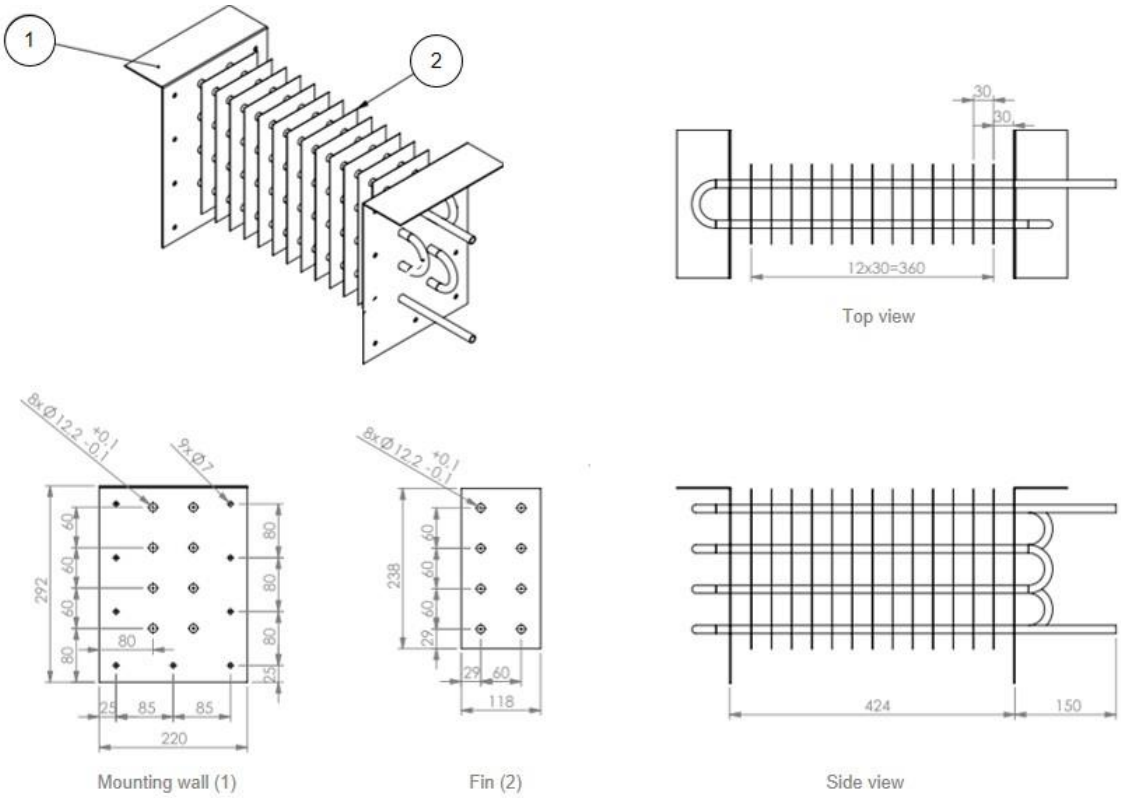

Figure 3. *The first heat exchanger – heat exchanger A.*

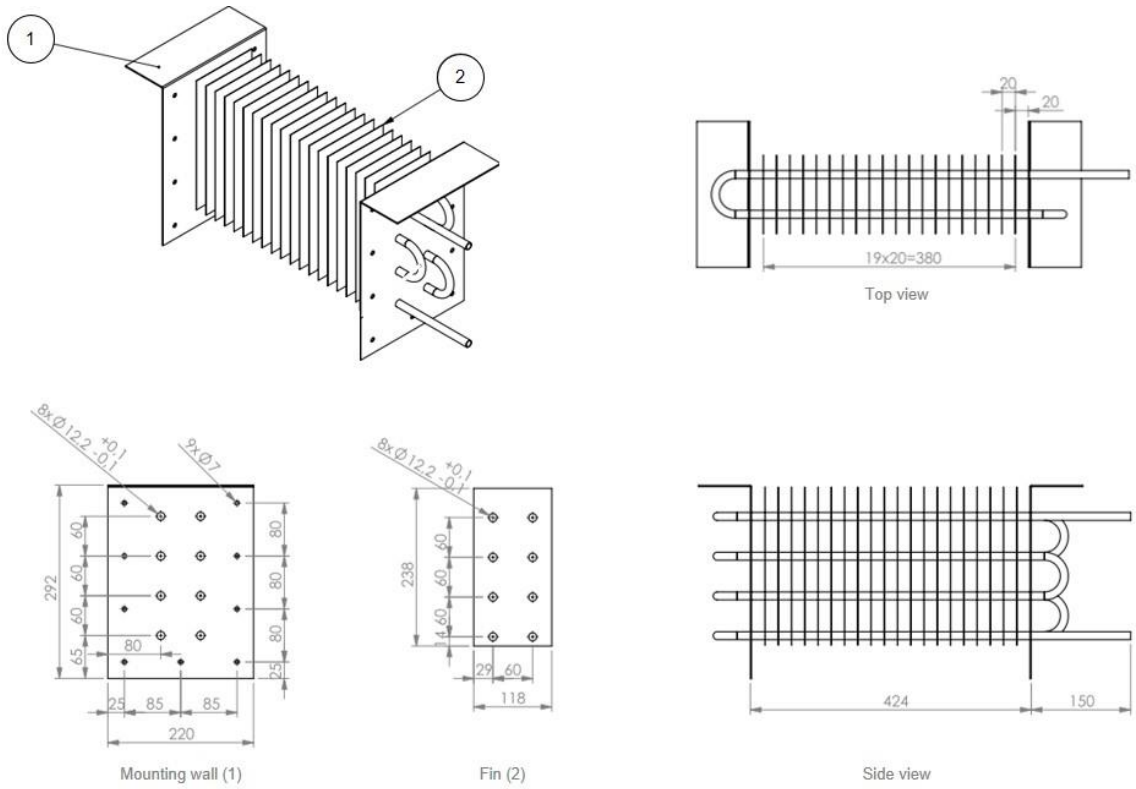

Figure 4. *The second heat exchanger – heat exchanger D.*

Table 1. *Measuring devices.*

Measured value	Device	Measuring range	Uncertainty
Temperature	Resistance temperature detector Pt100 TOP-PDm-98 (ALF-SENSOR sp. j., Zabierzów, Poland)	0 – 150 °C	$\pm(0{,}3+0{,}005\cdot\|t\|)$
Flow rate	Flow meter JUMO flowTrans MAG I02 (JUMO GmbH&Co. KG, Fulda, Germany)	0,2 – 10 m/s	±3,5% of measured value

3. Results and discussion

3.1. Heat exchanger A

The time dependence of the maximum (T_{max}), average (T_{avg}), and minimum (T_{min}) PCM temperatures measured in heat exchanger A during the charging and discharging processes is presented in **Figure 5a** and **Figure 5b**, respectively.

As observed, during the charging process, the initial T_{avg} was approximately 60 °C, regardless of the HTF flow rate. Subsequently, the temperatures T_{max}, T_{avg}, and T_{min} increased over time. The T_{max} was recorded at location 7 (see **Figure 2**), while the T_{min} was measured at location 6. The T_{max} rose rapidly, reaching a steady value of approximately 96 °C after about 2 hours from the start of the process. A similar T_{max} profile was observed for all three investigated flow rates, namely 2.4 L/min, 4.7 L/min, and 9.4 L/min. However, for the 4.7 L/min and 9.4 L/min cases, a sharp increase in T_{max} was observed approximately 10 minutes after the start of the measurements. This phenomenon can be attributed to volumetric shrinkage of the PCM during phase change. The PCM undergoes a significant volume decrease (approximately 20%) during solidification, leading to the formation of air gaps within the material, which is presented in **Figure 6**. Due to their much lower heat capacity, these air gaps heat up more rapidly than the surrounding PCM. Consequently, a temperature sensor located within such a gap may record a rapid temperature increase. When the surrounding PCM subsequently melts and fills the gap, the sensor becomes immersed in the colder (as compared to the air gap) PCM, resulting in a sudden drop in the recorded temperature.

Regarding T_{min}, a similar trend was observed for all three flow rates during the first three hours. Thereafter, T_{min} increased, until the target temperature of 92 °C was reached, more rapidly at lower flow rates. This result is unexpected and deviates from trends commonly reported in the literature. One possible explanation is

related to the configuration of the HTF inlet and outlet. The HTF inlet is located at the bottom of the heat exchanger (see **Figure 3**). As a result, the HTF temperature is highest at the bottom and decreases progressively along the flow path. At the lowest flow rate (2.4 L/min), the temperature gradient along the pipes is more pronounced compared to the higher flow rates (4.7 L/min and 9.4 L/min). Consequently, the upper region of the heat exchanger remains cooler, promoting natural convection within the molten PCM. In contrast, at higher flow rates, the temperature difference between the lower and upper sections is reduced, which suppresses buoyancy-driven flow and limits natural convection. Nevertheless, this hypothesis requires further experimental validation.

The temperature variations during the discharging process are presented in **Figure 5b**. The initial average temperature of the PCM within the heat exchanger was approximately 90 °C. Subsequently, T_{max}, T_{avg}, and T_{min} decreased gradually until T_{min} reached the target value of 70 °C. No significant differences were observed among the investigated flow rates.

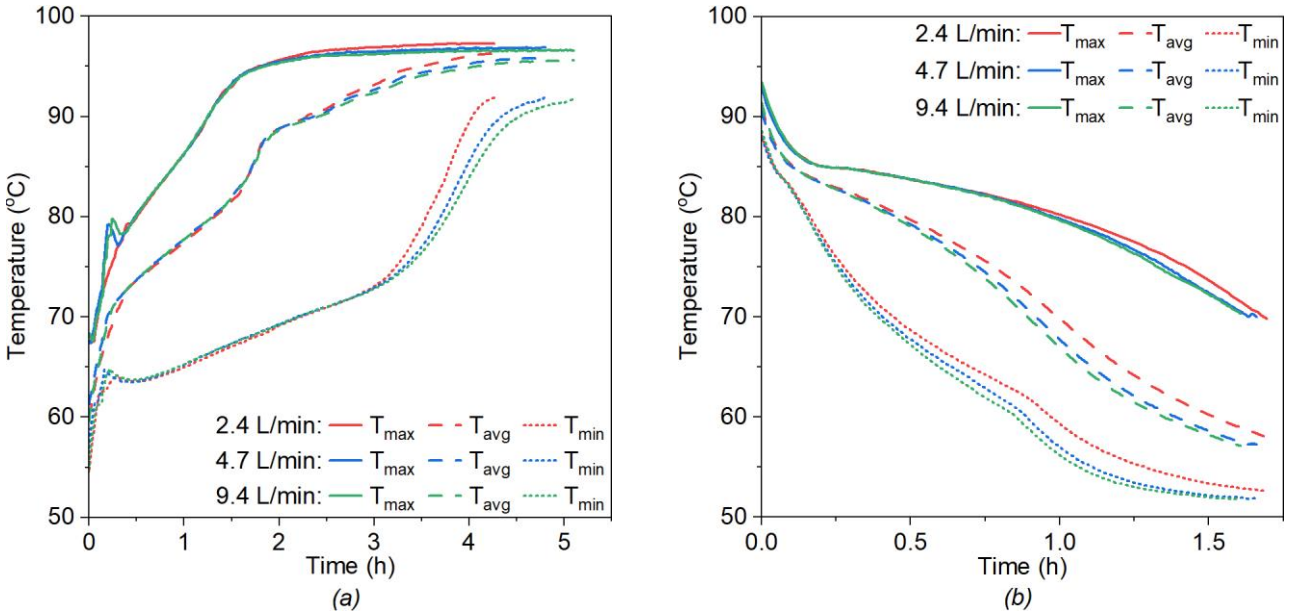

Figure 5. *The maximum (T_{max}), average (T_{avg}) and minimum (T_{min}) PCM temperature in heat exchanger A during: (a) charging; (b) discharging.*

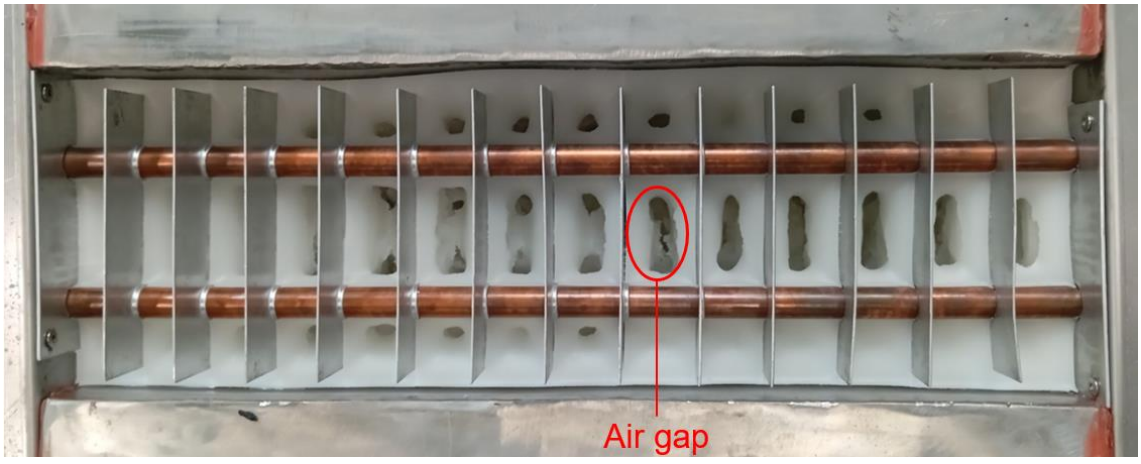

Figure 6. *Air gaps visible in the PCM in heat exchanger A.*

Figure 7a and **Figure 7b** present heat flow rate $\dot{Q}$, i.e., the thermal power of heat exchanger A, during the charging and discharging processes, respectively. The heat flow rate was calculated according to Eq. (1):

$$\dot{Q} = \dot{V} \cdot c_p \cdot \rho \cdot (T_{out} - T_{in}), \qquad (1)$$

where $\dot{V}$ is the measured volumetric flow rate (converted to m^3/s), c_p is the specific heat capacity of water (kJ/(kgK)), ρ is the density of water (kg/m^3), while T_{out} and T_{in} denote the measured outlet and inlet temperatures of the HTF (°C), respectively. The specific heat capacity and density of the water were taken from [14].

As observed, the highest heat flow occurs at the beginning of the process, with its absolute value reaching approximately 2.0 kW during both charging and discharging. Subsequently, the heat flow exhibits an

asymptotic behavior, characterized by a rapid initial change followed by a gradual approach toward a steady-state value of approximately 0 kW. No significant differences were observed among the investigated flow rates.

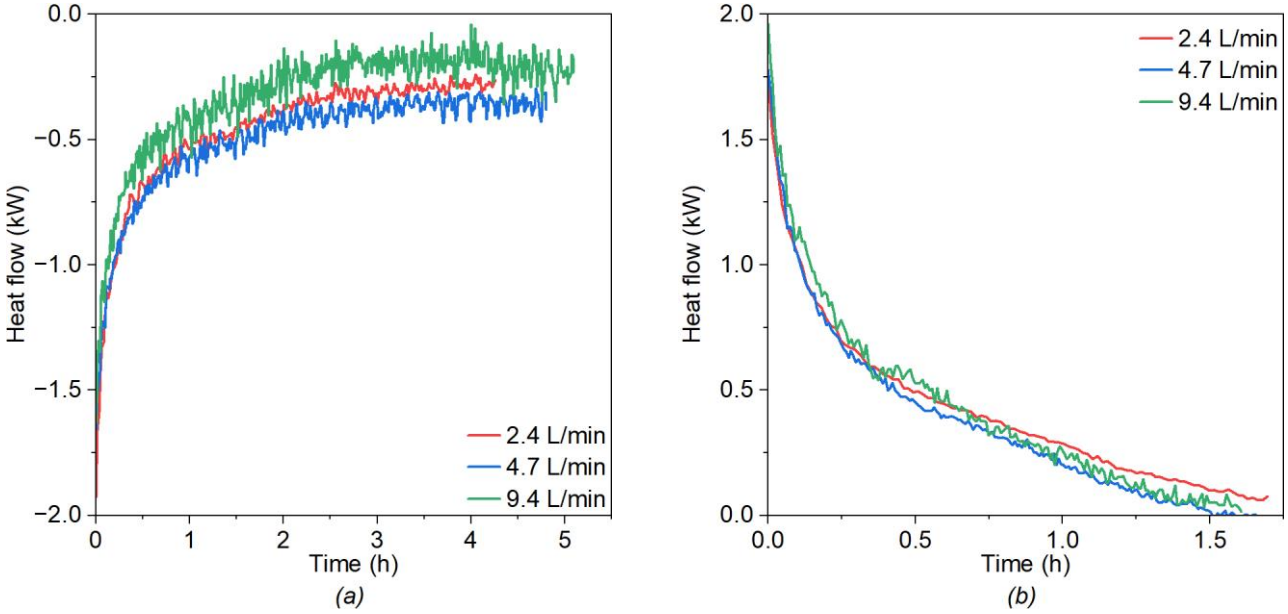

Figure 7. *The rate of heat flow in heat exchanger A during: (a) charging; (b) discharging.*

Figure 8 presents the charging and discharging times of the TES system equipped with heat exchanger A. As described in Section 2, the charging process was considered complete when T_{min} reached 92 °C, while the discharging process was assumed complete when T_{max} decreased to 70 °C.

As observed, in all investigated cases, the charging time is significantly longer than the discharging time. In contrast to findings commonly reported for PCM-based TES systems, the charging time increased with increasing HTF flow rate. A possible explanation for this behavior was discussed at the beginning of Section 3.1. As noted, this unexpected trend may result from the reduced temperature variation of the HTF along its flow path at higher flow rates, leading to a smaller temperature gradient across the height of the heat exchanger and, consequently, suppressed natural convection in the molten PCM.

The charging times were 4.3 h, 4.8 h, and 5.1 h for flow rates of 2.4 L/min, 4.7 L/min, and 9.4 L/min, respectively. In contrast, the discharging time decreased with increasing flow rate, amounting to 1.7 h, 1.63 h, and 1.60 h for the respective cases.

The observed differences in charging and discharging behavior – namely, the increase and decrease in duration with increasing flow rate – can be attributed to the dominant heat transfer mechanisms within the PCM. It is generally accepted that natural convection and conduction are the primary heat transfer mechanisms during melting (charging) and solidification (discharging), respectively [5].

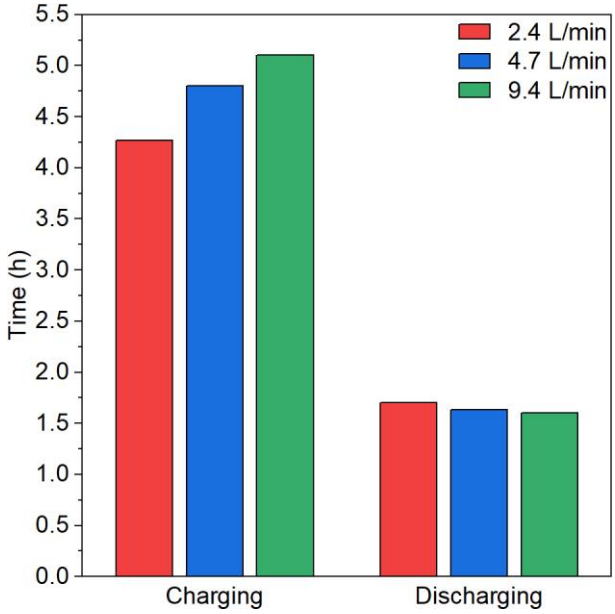

Figure 8. *The charging and discharging time in heat exchanger A.*

3.2. Heat exchanger D

The time dependence of the maximum (T_{max}), average (T_{avg}), and minimum (T_{min}) PCM temperatures measured in heat exchanger D during the charging and discharging processes is presented in **Figure 9a** and **Figure 9b**, respectively.

As observed, during the charging process, the initial T_{avg} was approximately 60 °C, regardless of the HTF flow rate. Subsequently, the temperatures T_{max}, T_{avg}, and T_{min} increased over time. The T_{max} was recorded at locations 2 and 3 (see **Figure 2**), while the T_{min} was measured at location 6. The T_{max} rose rapidly, reaching a steady value of approximately 96 °C after about 1.5 hours from the start of the process. A similar T_{max} profile was observed for all three investigated flow rates, namely 2.4 L/min, 4.7 L/min, and 9.4 L/min. In the case of heat exchanger D, no sharp increase in T_{max} at the beginning was observed, which can be attributed to the differences in the construction of those two heat exchangers (namely A and D).

Regarding the initial changes of T_{min}, a similar trends occurred in both, the 4.7 L/min and 9.4 L/min cases. A relatively rapid increase in the T_{min} is observed during first hour. In contrast, T_{min} in 2.4 L/min case increased slower at the beginning of the charging, however, after approximately 2 hours, T_{min} for the three investigated flow rates equalized. Then, T_{min} increased, until the target temperature of 70 °C is reached, more rapidly at lower flow rates. A possible reason for this unexpected result was explained in Section 3.1.

The temperature variations during the discharging process are presented in **Figure 9b**. The initial average temperature of the PCM within the heat exchanger was approximately 90 °C. Subsequently, T_{max}, T_{avg}, and T_{min} decreased gradually until T_{min} reached the target value of 70 °C. No significant differences were observed among the investigated flow rates.

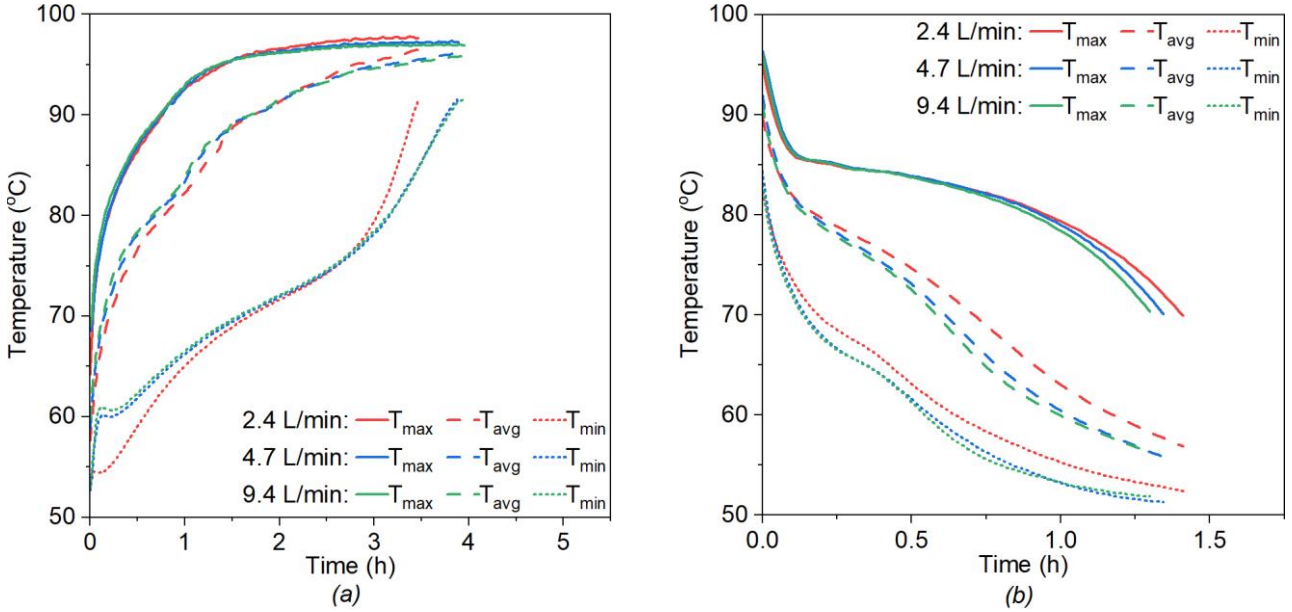

Figure 9. *The maximum (T_{max}), average (T_{avg}) and minimum (T_{min}) PCM temperature in heat exchanger D during: (a) charging; (b) discharging.*

Figure 10a and **Figure 10b** present heat flow rate $\dot{Q}$ (calculated according to Eq. (1)), i.e., the thermal power of heat exchanger D, during the charging and discharging processess, respectively. As observed, the highest heat flow occurs at the beginning of the process, with its absolute value reaching approximately 2.0 kW during both charging and discharging. Subsequently, the heat flow exhibits an asymptotic behavior, characterized by a rapid initial change followed by a gradual approach toward a steady-state value of approximately 0 kW. No significant differences were observed among the investigated flow rates.

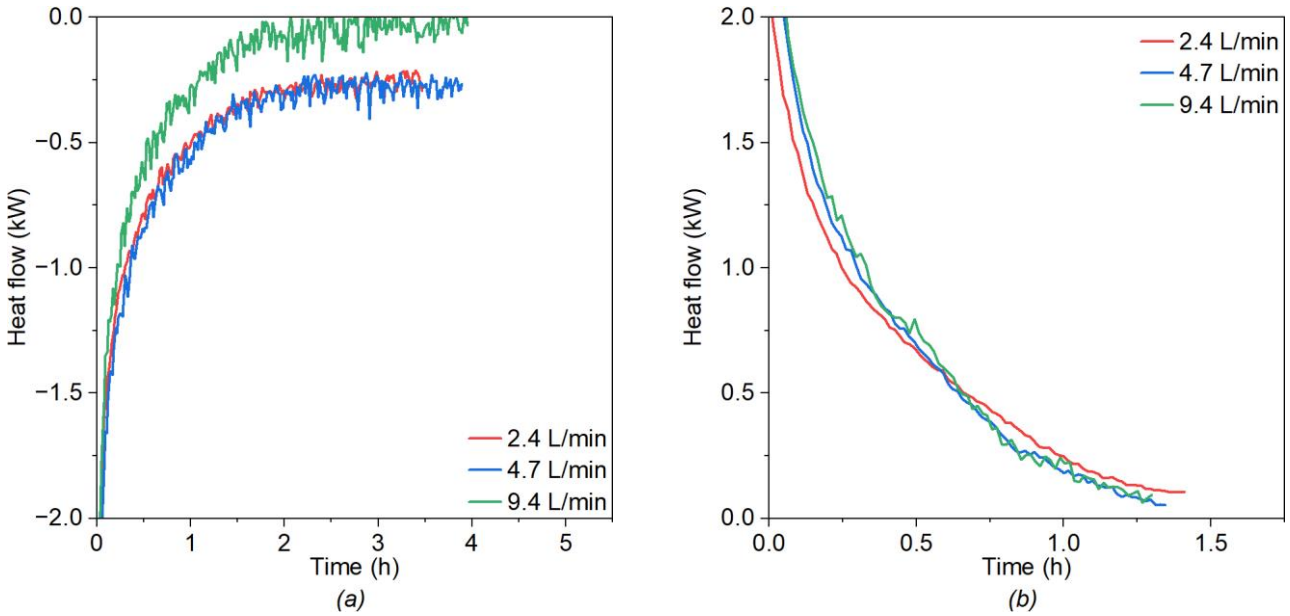

Figure 10. *The rate of heat flow in heat exchanger D during: (a) charging; (b) discharging.*

Figure 11 presents the charging and discharging times of the TES system equipped with heat exchanger D. As described in Section 2, the charging process was considered complete when T_{min} reached 92 °C, while the discharging process was assumed complete when T_{max} decreased to 70 °C.

As observed, in all investigated cases, the charging time is significantly longer than the discharging time. In contrast to findings commonly reported for PCM-based TES systems, the charging time increased with increasing HTF flow rate. A possible explanation for this behavior was discussed at the beginning of Section 3.1. As noted, this unexpected trend may result from the reduced temperature variation of the HTF along its flow path at higher flow rates, leading to a smaller temperature gradient across the height of the heat exchanger and, consequently, suppressed natural convection in the molten PCM.

The charging times were 3.5 h, 3.9 h, and 4.0 h for flow rates of 2.4 L/min, 4.7 L/min, and 9.4 L/min, respectively. In contrast, the discharging time decreased with increasing flow rate, amounting to 1.42 h, 1.35 h, and 1.30 h for the respective cases.

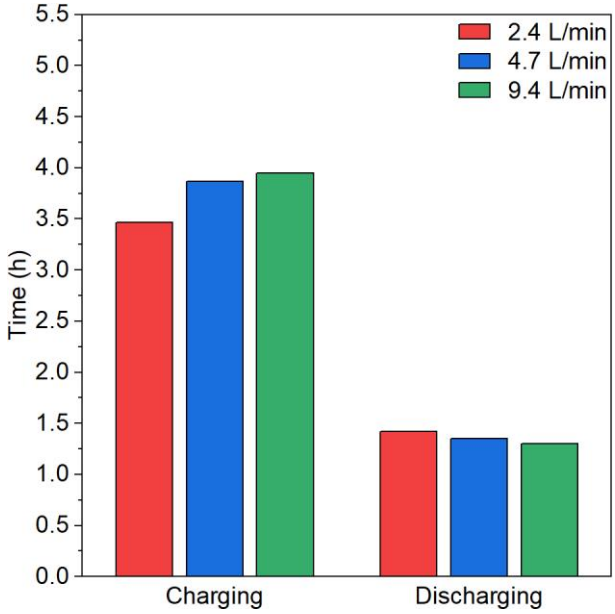

Figure 11. *The charging and discharging time in heat exchanger D.*

4. Conclusions

In this study, two PCM-based TES systems were investigated. The systems differed in the design of their heat exchangers: heat exchanger A was equipped with fourteen straight alumina fins, whereas heat exchanger D incorporated twenty-one straight alumina fins along with HTF tubes positioned 15 mm lower. In both cases, 10 kg of a commercially available PCM, A82 (Phase Change Material Products Limited, UK), was used. The

primary objective of this study was to evaluate the effect of HTF flow rate on the performance of the two TES systems. The HTF flow rates were set at 2.4 L/min, 4.7 L/min, and 9.4 L/min, corresponding to average flow velocities of 0.5 m/s, 1.0 m/s, and 2.0 m/s, respectively.

The results indicate that, for heat exchanger A, the charging times were 4.3 h, 4.8 h, and 5.1 h at flow rates of 2.4 L/min, 4.7 L/min, and 9.4 L/min, respectively. For heat exchanger D, the corresponding charging times were shorter, amounting to 3.5 h, 3.9 h, and 4.0 h. These results are unexpected and deviate from trends commonly reported in the literature, where higher flow rates typically enhance heat transfer and reduce charging time. One possible explanation for this behavior lies in the configuration of the HTF flow path and the resulting temperature distribution. The HTF inlet and outlet were located at the bottom and top of the heat exchanger, respectively. As the HTF flow rate increases, the temperature gradient along the height of the heat exchanger decreases, leading to nearly uniform temperatures between the lower and upper regions. This effect may suppress natural convection in the molten PCM. However, this hypothesis requires further experimental validation. It was also observed that the discharging times were approximately 2.5 – 3.2 times shorter than the charging times. For heat exchanger A, the discharging times were 1.70 h, 1.63 h, and 1.60 h for flow rates of 2.4 L/min, 4.7 L/min, and 9.4 L/min, respectively. For heat exchanger D, the corresponding values were 1.42 h, 1.35 h, and 1.30 h.

The study also identified several technical challenges associated with PCM-based TES systems. One notable issue is the volumetric shrinkage of the PCM during phase change, which leads to the formation of air gaps. These gaps can significantly hinder heat transfer within the material. Despite these challenges, PCM-based TES systems remain a promising solution for thermal energy storage and warrant further investigation.

Acknowledgments

This research was mainly supported by The National Centre for Research and Development, Poland - project “Opracowanie mobilnego magazynu ciepła pozwalaj ¸acego na wykorzystanie ciepła odpadowego dla spółki PTEP” Nowe Technologie w Zakresie Energii II (NTE-II/0004/2022), and partially supported by the Ministry of Science and Higher Education, Poland, grant AGH number 16.16.210.476.

Nomenclature

Symbols

c_p	specific heat capacity, kJ/(kg K)
$\dot{Q}$	heat flow rate, kW
$\dot{V}$	volumetric flow rate, m^3/s
T	temperature, °C

Greek symbols

ρ	density, kg/m^3

Subscripts and superscripts

in	inlet
out	outlet

References

[1] Vallese L, Javadi H, Badenes B, Urchueguia JF, Lombardo G, Menegazzo D, et al. A comprehensive review of thermal energy storage technologies and their applications: Creation of a database. Renew Sustain Energy Rev 2026;225:116133. https://doi.org/10.1016/j.rser.2025.116133.

[2] Hekimoğlu G, Sarı A. A review on phase change materials (PCMs) for thermal energy storage implementations. Mater Today Proc 2022;58:1360–7. https://doi.org/10.1016/j.matpr.2022.02.231.

[3] Rolka P, Przybylinski T, Kwidzinski R, Lackowski M. Investigation of low-temperature phase change material (PCM) with nano-additives improving thermal conductivity for better thermal response of thermal energy storage. Sustain Energy Technol Assessments 2024;66:103821. https://doi.org/10.1016/j.seta.2024.103821.

[4] Xu X, Zhang X, Ji J, Fang M, Yang M, Ma K, et al. Comparative Analysis of Additives for Increasing Thermal Conductivity of Phase Change Materials: A Review. Energy & Fuels 2022;36:5088–101. https://doi.org/10.1021/acs.energyfuels.2c00522.

[5] Radomska E, Mika L, Sztekler K, Lis L. The Impact of Heat Exchangers’ Constructions on the Melting and Solidification Time of Phase Change Materials. Energies 2020;13:4840. https://doi.org/10.3390/en13184840.

[6] Peng Q, Luo Y, Sun X, Li J, Chen Y, Dang C. Study on the effects of heat transfer fluid (HTF) temperature and flow velocity on energy storage/release performance of shell and tube phase change heat exchanger. J Energy Storage 2025;107:114935. https://doi.org/10.1016/j.est.2024.114935.

[7] Herbinger F, Groulx D. Experimental comparative analysis of finned-tube PCM-heat exchangers' performance. Appl Therm Eng 2022;211:118532. https://doi.org/10.1016/j.applthermaleng.2022.118532.

[8] Niu L, Xing G, Huo Z, Liu Y, Liu C. Model experiment and numerical study on the heat storage law of phase change material in different heat transfer structures. J Energy Storage 2025;120:116457. https://doi.org/10.1016/j.est.2025.116457.

[9] Fan K, Zong S, Gao H, Duan Z. Experimental Study on Thermal Performance of PCM in an Inclined Shell-and-Tube Latent Heat Thermal Energy Storage Unit. Processes 2025;13:1557. https://doi.org/10.3390/pr13051557.

[10] Lv L, Huang S, Zou Y, Wang X, Zhou H. Heat transfer and thermal resistance analysis under various heat transfer fluid flow rates based on a medium-temperature pilot-scale latent heat storage system. Int J Heat Mass Transf 2024;220:124896. https://doi.org/10.1016/j.ijheatmasstransfer.2023.124896.

[11] Panchabikesan K, Swami M V., Ramalingam V, Haghighat F. Influence of PCM thermal conductivity and HTF velocity during solidification of PCM through the free cooling concept – A parametric study. J Energy Storage 2019;21:48–57. https://doi.org/10.1016/j.est.2018.11.005.

[12] Shen G, Wang X, Yu J, Bin Y, Zhong S, Yang S, et al. Experimental investigation of thermal performance of vertical multitube cylindrical latent heat thermal energy storage systems. Environ Sci Pollut Res 2024;31:46447–61. https://doi.org/10.1007/s11356-024-31864-7.

[13] PCM Products 2026. https://www.pcmproducts.net/ (accessed April 10, 2026).

[14] Kretzschmar H-J, Wagner W. International Steam Tables. Berlin, Heidelberg: Springer Berlin Heidelberg; 2019. https://doi.org/10.1007/978-3-662-53219-5.